Effects of site substitution and metal ion addition on doped manganites

2002 J. Phys.: Condens. Matter 14 10323

(http://iopscience.iop.org/0953-8984/14/43/328)

INSTITUTE OF PHYSICS PUBLISHING JOURNAL OF PHYSICS: CONDENSED MATTER

J. Phys.: Condens. Matter **14** (2002) 10323–10329 PII: S0953-8984(02)37663-X

Effects of site substitution and metal ion addition on doped manganites

A K Pradhan[1], Y Feng[2], B K Roul[3], D R Sahu[3] and M Muralidhar[4]

[1] Jesse W Beams Laboratory of Physics, University of Virginia, Charlottesville, VA 22901, USA
[2] Northwest Institute for Nonferrous Metal Research, PO Box 51, Xi'an 710016, People's Republic of China
[3] Institute of Materials Science, 68/1 Laxmi Vihar, Bhubaneswar 751005, India
[4] SRL/ISTEC, 1-10-13 Shinonome, Koto-ku, Tokyo 135-0062, Japan

E-mail: akp4x@virginia.edu

Received 5 June 2002, in final form 31 July 2002
Published 18 October 2002
Online at stacks.iop.org/JPhysCM/14/10323

Abstract

We report transport, magnetization and transmission electron microscopy studies of the effects of A- and B-site substitution, and the addition of metal ions such as Pt, Ag and Sr, on doped ABO_3 perovskites, where A = La, Pr etc and B = Mn. Disorder induced by such substitution changes the behaviour of the charge-ordered (CO) state significantly. A- and B-site substitution suppresses the CO phase due to size mismatch and disorder produced by inhomogeneity. On the other hand, addition of metal ions such as Pt and Ag improves several colossal-magnetoresistance properties significantly due to microstructural effects and enhanced current percolation through grain boundaries.

The recent intensive research on perovskite manganites has revealed many new aspects in the area of strongly correlated electron systems [1]. These materials are insulators at high temperature (T) and transform into bad metals at low T when cooled through a metal–insulator transition temperature (T_{MI}). At T_{MI}, a peak in the resistivity ρ appears and separates the insulator from the ferromagnetic (FM) region. Interestingly, application of a magnetic field turns the insulator into a metal in the vicinity of T_{MI}—exhibiting a large 'colossal magnetoresistance' (CMR). At high T ($T \geqslant T_{MI}$), a paramagnetic insulator, at intermediate T ($T \cong T_{MI}$), a charge-ordered (CO) state [2] with CMR and, at low T ($T \leqslant T_{MI}$), an FM metallic phase are generally seen in doped rare-earth manganites. The CMR properties appear to be associated with the coexistence of intrinsic sub-micron scale inhomogeneities of two competing phases consisting of the CO phase [2] and an FM metallic phase. This can be consistently explained using the recently developed concept of phase separation (PS) [2] due to inhomogeneities, induced by Mn oxides in combination with percolation [3, 4], taking into account the phenomenological model of a random resistor network. As CMR materials

are becoming increasingly important as potential candidates for use in several applications including as high-T infrared detectors, bolometers, magnetic memories and sensors, tailoring of the materials using different substitution schedules and understanding the underlying mechanism remain extremely important.

In this paper, we report transport, magnetization and transmission electron microscopy (TEM) studies of the effects of A- and B-site substitution, and the addition of metal ions such as Pt, Ag and Sr, on doped ABO_3 perovskites, where A is a rare earth (La, Nd etc) and B is Mn. Disorder induced by such substitution significantly changes the behaviour of the CO state. A- and B-site substitution suppresses the CO phase due to size mismatch and disorder due to inhomogeneity. On the other hand, addition of metal ions improves several CMR properties significantly due to microstructural effects and improved percolation.

A series of high-quality samples of Ho-, Nd-, Cr- and Sr-doped $La_{0.67}Ca_{0.33}MnO_3$ (LCMO) and $Pr_{0.5}Ca_{0.5}MnO_3$ (PCMO) was prepared by the melt-processing (MP) technique [5]. The doping was done either at A or B sites as described later. Pt and Ag were added to some of the above samples to study the influence of metal ions on the matrix. The x-ray diffraction patterns show single-phase material. A standard four-probe ac technique ($f = 17$ Hz, $I = 0.1$ mA rms) was used to measure the magnetoresistance. The zero-field-cooled (ZFC) and field-cooled (FC) measurements of the magnetization (M) were carried out down to 5 K using a superconducting quantum interference device magnetometer (Quantum Design).

Figure 1(a) shows the resistivity of LCMO at $H = 0$ for La-site substitution of Ho and Nd, Ca-site substitution of Sr and excess addition of Ag and Ho to stoichiometric LCMO. A fairly sharp transition is recorded with $T_{MI} \sim 262$ K for LCMO, whereas significant change in the resistivity occurs for a small amount of Ho substitution at the La site. T_{MI} is dramatically suppressed, mainly due to decrease in the tolerance factor. On the other hand, although Nd substitution at the La site and excess addition of Ho do not change T_{MI}, the resistivity falls much more gradually in the FM state. This behaviour clearly indicates that the magnetic inhomogeneity and disorder suppress the CO state. We note that T_{MI} is very sensitive to the processing temperature and conditions. This may be one of the causes of a slight increase of T_{MI} in our Nd-substituted sample compared to LCMO. We suspect that the microscopic grain connectivity in our Nd-substituted sample is better than that of LCMO. This may be due to slight alteration in the processing schedule. The transition widths for the Nd- and Ho-substituted samples are large. However, the FM state in the Ho-doped sample is more homogeneous than that in the Nd-doped sample for the same level of substitution. A large decrease in T_{MI} for Ho-doped LCMO is not understood clearly. One of the reasons may be due to the decrease in the tolerance factor of the Ho-doped sample compared to that for the Nd-doped sample. For Ca-site substitution of Sr, T_{MI} is enhanced; however, the CO region is again suppressed. Surprisingly, the addition of Ag enhances T_{MI} significantly without there being much change in the CO state, like that observed in thin-film samples [6]. Hence the metal ion substitution either at the Ca site or as a separate addition to the matrix seems promising for enhancing T_{MI} without causing much damage to the CO state. Our results are consistent with the recent proposal [7] in which it is predicted that an optimum value of nonmagnetic disorder favours the CMR effect.

In order to illustrate further the effects of metal ions on the transition, we show the zero-field resistivity of $(La_{0.335}Ho_{0.335})Sr_{0.33}MnO_3$ and a sample with 0.5 mol% Pt prepared under the same conditions in figure 1(b). The metal–insulator transition is enhanced by about 25 K on Pt addition, indicating the strong influence on the transition as observed for the Ag addition. This is further confirmed by the FC and ZFC magnetization behaviour presented in figure 2 for two samples with and without Pt addition, which will be discussed later. However, addition of further Ho at the La site (the results are shown in figure 1(b) as curves 3) displays an

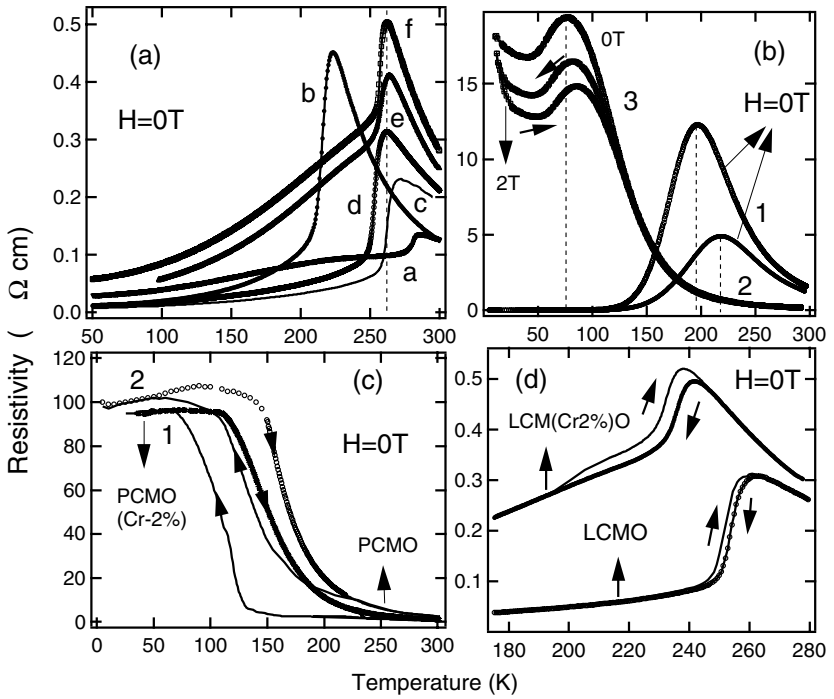

Figure 1. The temperature dependence of the resistivity for (a) a: $La_{0.67}Ca_{0.297}Sr_{0.033}MnO_3$ (LCSM); b: $(La_{0.64}Ho_{0.03})Ca_{0.33}MnO_3$; c: $La_{0.67}Ca_{0.33}MnO_3$ (LCM) with 1 mol% Ag; d: LCM; e: $(La_{0.64}Nd_{0.03})Ca_{0.33}MnO_3$; f: $La_{0.64}Ca_{0.33}MnO_3$ with 2 mol% Ho for $H = 0$; (b) 1: $(La_{0.335}Ho_{0.335})Sr_{0.33}MnO_3$ and 2: with 0.5 mol% Pt in zero field; 3: $(La_{0.17}Ho_{0.5})Sr_{0.33}MnO_3$ for zero-field warming and cooling, and warming and cooling in a field of 2 T; (c) 1: PCMO; 2: $Pr_{0.5}Ca_{0.5}Mn_{0.98}Cr_{0.02}O_3$ in zero field; (d) LCMO and $La_{0.67}Ca_{0.67}Mn_{0.98}Cr_{0.02}O_3$ in zero field exhibiting hysteresis. The arrows indicate the T-cycling during the cooling and warming.

unusual resistivity behaviour for $(La_{0.17}Ho_{0.5})Sr_{0.33}MnO_3$ in zero field. The thermal cycling of the resistivity in a field of 2 T exhibits significant hysteresis in the metal–insulator transition regime. The unusual upturn of the resistivity both in zero field and in a field may be related to the localization of charge carriers due to the presence of AFM clusters. Alternatively, similar upturn behaviour of the resistivity can also be explained as a signature of disordered metallic systems [8].

In figures 1(c) and (d), we show the effects of 2 mol% Cr doping at the Mn site on the zero-field resistivity of PCMO and LCMO—yielding significant hysteresis on thermal cycling. T_{c0} for the Cr-doped sample is about 25 K higher to that of PCMO. The most remarkable feature is that the hysteresis in the resistivity of PCMO is somewhat symmetric in contrast to the asymmetric hysteresis in Cr-doped PCMO. Our results are different to those in another report [9] in which a clear T_{M1} is seen for Cr-doped PCMO. Furthermore, the resistivity curve for PCMO in [9] is different to ours. Although the staring stoichiometry of Cr was taken as 2% for the melt processing, the transition for our Cr-doped PCMO is very similar to that in the recent report [10] for Cr = 1.5%. The actual causes of these discrepancies are not known yet. However, the evolution of a large hysteresis in thermal cycling in the Cr-doped sample is reminiscent of the scenario for a state with increased charge ordering. Further microscopic studies are warranted for these melt-processed samples, to provide a better

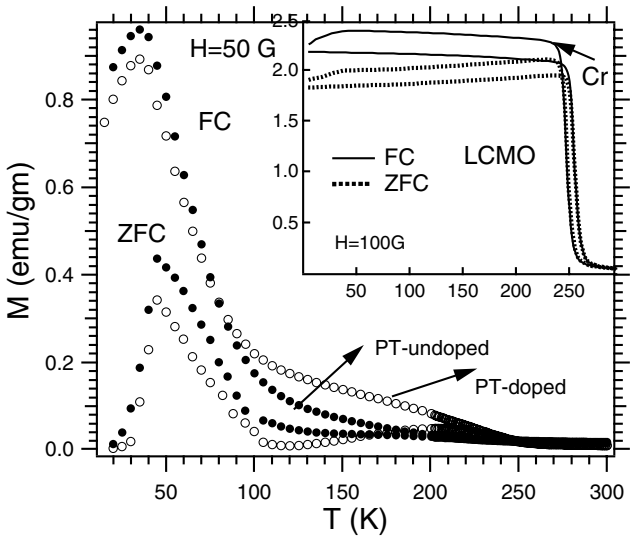

Figure 2. The temperature-dependent magnetization of $(La_{0.335}Ho_{0.335})Sr_{0.33}MnO_3$ and that for a sample with 0.5 mol% Pt doping for ZFC and FC samples at $H = 5$ mT. The inset shows FC and ZFC magnetization of LCMO and Cr-doped LCMO.

understanding of their physical behaviour. On the other hand, a distinct first-order transition along with a small hysteresis is observed in LCMO with temperature cycling in the CO region. T_{c0} for the Cr-doped LCMO sample is slightly pushed back towards the lower-temperature region. However, a remarkably elongated hysteresis is observed in Cr-doped LCMO. The sharp first-order transition observed in LCMO is transformed into a rapid crossover in Cr-doped LCMO, indicating the formation of clusters. In contrast, although T_c is slightly reduced on Cr doping, the nature of the transition is not very much affected except at low temperature in the temperature-dependent FC and ZFC magnetization shown in the inset of figure 2. This is very similar to the recent report [11] of effects of Cr on LaSrMnO, in which cluster-glass behaviour was observed with increasing Cr at the Mn site. However, the value of the magnetization increases on Cr doping, indicating the possibility of an FM superexchange interaction. On the other hand, it is obvious that we should consider the Mn^{3+}–O–Cr^{3+} double-exchange (DE) phenomena [12], due to the identical electronic configurations of Cr^{3+} and Mn^{4+}. However, the situation remains much more complicated, although it still appears promising to attempt to tune the CMR by Mn-site doping of other foreign elements [13, 14].

It is certain that Cr introduces some degree of disorder in the Mn sublattice [15] as well as in the matrix. We also consider that Cr (as well as Mn) introduces nanometre scale clusters in addition to causing the formation of small Mn^{3+}–O–Cr^{3+} groups that coexist with Mn^{3+}–O–Mn^{4+} groups, yielding interesting transport properties. These nanoclusters (FM or AFM depending on the doping level) and disorders can be frozen along with the spin-glass behaviour in random directions. Hence, we believe that the weakening of the CO–AF ground state by Mn-site doping in manganite is induced by disorder from the Mn sublattice. However, a small amount of Mn-site substitution of Cr could increase the temperature regime for the existence of the CO phase, which may be beneficial for applications.

Now we discuss the microscopic evidence for the disorders caused by the site substitution and metal ion addition. In the top left inset of figure 3, we show the electron diffraction of La(Ca, Sr)MnO exhibiting superlattice spots clearly. This signifies that the CO state is

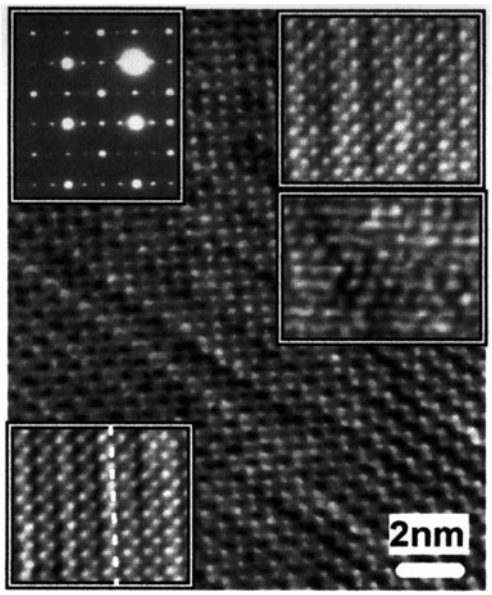

Figure 3. A high-resolution TEM image of LCSM is shown. The top left inset shows the electron diffraction patterns at 290 K indicating superlattice spots. The top right upper and lower and the bottom left images are enlarged views of regions in the selected area. The dotted line in the bottom inset shows a typical anti-phase boundary.

incommensurate. However, the satellite peaks are not exactly the same as those seen in LCMO, reported earlier [5], but are slightly inclined. The modulation period changes due to cation size mismatch and disorder even with a small amount of substitution of Sr at the Ca site. This kind of disorder can suppress the CO state. In this case, the partial destruction of the CO state cannot be attributed to the commensurate ratio of Mn^{4+} and Mn^{3+} as was the case for other samples with Cr substitution. The distinguishing feature is the change in the commensurate modulation (presented in figure 3) from those from high-resolution electron microscopy (HREM) studies. There are several interesting features observable in figure 3. The ordered cells are not perfectly regular in all places. Defective cells in many places disrupt the sequences of the orbital cells as shown in the top right (upper) inset of figure 3 on an enlarged scale. The distortions due to disorders are distinctly visible in the HREM image presented in the top right (lower) inset. The original periodicity is disturbed due to discommensuration introduced by size mismatch and resulting disorder. We argue that the disorder created by the similar size mismatch is one of the most significant reasons for suppression of the CO state in all substitutions. A similar conclusion was drawn recently from the microscopic observation of A-site cation substitution [16].

Another significant observation is the anti-phase boundary in a selected region of figure 3 (such features are very often found in manganites [2, 5]) shown as a dotted line in the bottom left inset of figure 3. The phase difference between the two sides of such a boundary is π. The periodicity of these boundaries remains almost unchanged when a small degree of disorder is introduced. This signifies that the presence of anti-phase boundaries is an intrinsic property for all manganites exhibiting CMR properties.

Spin polarization through grain boundaries (GBs) remains one of the most important phenomena in manganites. In order to illustrate the influence of metal ions on the above effects,

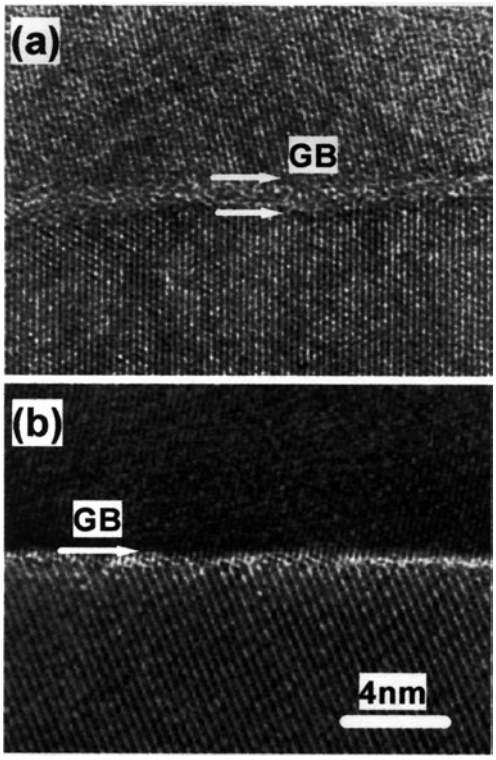

Figure 4. Transmission electron images of Ag-doped LCM showing (a) broad GBs and (b) narrow GBs. The arrows indicate the boundary regions.

we show two remarkable types of GB in figure 4 obtained from our TEM images, taken for an Ag-doped LCMO sample in two selected regions. The broad boundary of figure 4(b) is due to the disorder induced by Ag that agglomerates at the boundary and facilitates current percolation. Generally, LCMO is viewed as a random resistor network through which conduction occurs by percolation [3, 4]. The MR change in the CO state is related to the small spin polarization in the FM region that enhances conductivity between the metallic domains. Furthermore, it has been shown that grain connectivity and spin polarization through GBs [5, 17] enhance conductivity significantly, and produce three major effects: (a) shift of T_{MI} closer to T_c; (b) sharpening of T_c; and (c) decrease in the resistivity. Therefore, the resistance of the insulating PM region, R_I, and that of the metallic FM region, R_M, grow simultaneously until T approaches T_{MI}, where the metallic filament-like percolating paths start melting down. This is one of the major reasons for the enhanced conductivity and T_{MI} of manganites when metal ions are doped in, irrespective of the introduction of additional disorders which are thought to suppress the CO state. These metal ions establish a current homogeneity and enhanced percolating network in the sample. These studies show that there remain several ways to tune and improve the CMR properties significantly for applications at room temperature.

Summarizing, we have reported transport, magnetization and TEM studies of the effects of different site substitutions, and the addition of metal ions such as Pt, Ag and Sr, on doped ABO_3 manganites. Disorder induced by such substitutions significantly changes the behaviour of the CO state. A- and B-site substitution suppresses the CO phase due to size mismatch and disorder caused by inhomogeneity. On the other hand, addition of metal ions improves several

CMR properties significantly due to microstructural effects and enhanced current percolation through grain boundaries.

References

[1] Tokura Y and Nagosa N 2000 *Science* **288** 462
[2] Uehara M, Mori S, Chen C H and Cheong S-W 1999 *Nature* **399** 560
[3] Mayr M, Moreo A, Verges J A, Arispe J, Feiguin A and Dagotto E 2001 *Phys. Rev. Lett.* **86** 135
[4] Moreo A, Mayr M, Feiguin A, Yunoki S and Dagotto E 2000 *Phys. Rev. Lett.* **84** 5568
[5] Pradhan A K, Roul B K, Feng Y, Wu Y, Mohanty S, Sahu D and Dutta P 2001 *Appl. Phys. Lett.* **78** 1598
Pradhan A K, Roul B K, Feng Y, Wu Y, Mohanty S, Sahu D and Dutta P 2000 *Appl. Phys. Lett.* **76** 763
[6] Shreekala R, Rajeswari M, Pai S P, Lofland S E, Ogale S B, Bhagat S M, Downes M J, Greene R L, Ramesh R and Venkatesan T 1999 *Appl. Phys. Lett.* **74** 2857
[7] Sheng L, Xing D Y, Sheng D N and Ting C S 1997 *Phys. Rev. Lett.* **79** 1710
[8] Barman A, Ghosh S, Biswas S, De S K and Chatterjee S 1998 *Solid State Commun.* **106** 691
[9] Raveau B, Maignan A and Martin C 1997 *J. Solid State Chem.* **130** 162
[10] Mahendiran R, Raveau B, Hervieu M, Michel C and Maignan A 2001 *Phys. Rev.* B **64** 064424
[11] Sun Y, Tong W, Xu X and Zhang Y 2001 *Appl. Phys. Lett.* **78** 643
[12] Barnabe A, Maignan A, Hervieu M, Damay F, Martin C and Raveau B 1997 *Appl. Phys. Lett.* **71** 3907
[13] Ghosh K, Ogale S B, Ramesh R, Greene R L, Venkatesan T, Gapchup K M, Bathe R and Patil S I 1999 *Phys. Rev.* B **59** 533
[14] Maignan A, Damay F, Barnabe A, Martin C, Hervieu M and Raveau B 1998 *Phil. Trans. R. Soc.* A **356** 1635
[15] Rivadulla F, Lopez-Quintela M A, Hueso L E, Sande P, Rivas P J and Sanchez R D 2000 *Phys. Rev.* B **62** 5678
[16] Wang Q Y, Duan X F, Wang Z H and Shen B G 2001 *Appl. Phys. Lett.* **78** 2157
[17] de Andrés A, García-Hernández M, Martínez J L and Prieto C 1999 *Appl. Phys. Lett.* **74** 3884